

# Enabling Eutectic Soldering of 3D Opto-Electronics onto Low Tg Flexible Polymers

*Meriem Ben Salah Ep Akin  
Lutz Rissing  
Wolfgang Heumann*



Electrical Engineering and Computer Sciences  
University of California at Berkeley

Technical Report No. UCB/EECS-2014-53

<http://www.eecs.berkeley.edu/Pubs/TechRpts/2014/EECS-2014-53.html>

May 3, 2014

Copyright © 2014, by the author(s).  
All rights reserved.

Permission to make digital or hard copies of all or part of this work for personal or classroom use is granted without fee provided that copies are not made or distributed for profit or commercial advantage and that copies bear this notice and the full citation on the first page. To copy otherwise, to republish, to post on servers or to redistribute to lists, requires prior specific permission.

#### Acknowledgement

The authors gratefully acknowledge the financial support by Deutsche Forschungsgesellschaft (DFG) within the Collaborative Research Center “Transregio 123-Planar Optronic Systems.”

Moreover, the authors would like to acknowledge Prof. Schade and Elke Pichler from the Institute of Energy Research and Physical Technologies at the Technical University of Clausthal for coordinating the measurements of the coefficients of thermal expansion.

# Enabling Eutectic Soldering of 3D Opto-Electronics onto Low Tg Flexible Polymers

Meriem Akin, Lutz Rissing, Wolfgang Heumann

## Abstract

We present a cost-efficient and reproducible technique for assembling 3D components to mechanically bendable low glass transition temperature (T<sub>g</sub>) polymeric interposers. First, we propose localized soldering using a focused hot air gun. Second, we use eutectic solders, which permit reflow at temperatures close to the T<sub>g</sub> of the interposer. Then, we adopt differential heating and cooling in order to enable rapid heat dissipation through the interposer during soldering. Furthermore, we apply a metal jig as a load to maintain contact between the interposer and the 3D component during soldering. Also, the jig serves as a shield to protect the interposer surface outside the soldering zone from thermal loading, and more importantly as a passive heat sink. We showcase our approach by manufacturing a test vehicle on a polyethylene terephthalate (PET) interposer having a T<sub>g</sub> of 71 deg. C. We solder a 30 mA DC current SMD LED by means of a eutectic compound of 48 w. % Sn and 52 w. % In at 118 deg. C.

## Related Work

As the world is moving towards the internet of everything, smart structures, e.g. mechanically bendable opto-electronic sensors, will be mounted everywhere to serve night and day. That being the case, and in order to solve the bottleneck associated with the manufacturing cost of the next generation of smart structures, ultra low-cost organic materials like lightweight polymers at the interposer or component level are to be employed. Currently, lightweight inexpensive polymers like polyethylene terephthalate (PET), polycarbonate (PC), polymethyl methacrylate (PMMA) and polyvinyl chloride (PVC) are dedicatedly employed in numerous applications such as RFID tagging [2], medical implants [5] and electronic displays [1]. Thereupon, polymeric substrates offering a wide range of optical, thermal and mechanical properties are researched and manufactured [8]. Moreover, the use of the aforementioned polymers as a platform for the deposition of electronic interconnects is extensively investigated ([3], [4], [6], [9], [16]).

Nonetheless, practices of surface mounting of three-dimensional (3D) components to the deposited interconnects remain limited due to the restricted thermal budgets of the substrate. Clearly, inexpensive polymers like PET, PC, PMMA and PVC have glass transition temperatures (T<sub>g</sub>) below 150 deg. C. Low rigidity and thermal sensitivity of these aforementioned polymers at classically low temperatures constitute the brainteaser. In order to ensure an effective roll-to-roll mass production, warpage of the polymer interposer that is due to coefficient of thermal expansion (CTE)

mismatches of the assembly and thermo-mechanical properties of the interposer need to be monitored rigorously.

While low heat thermo-compressive ([10], [12]) or ultraviolet adhesive bonding [13] comply with the thermal budget of the substrate, limitations on the shear strength and electrical resistivity of the adhesive joint persist. Hence, various non-ceasing efforts on adapting conventional surface mount technologies such as thermal soldering to inexpensive polymers are expended. For instance, recent investigations on sintering Ag-based solder pastes onto PC substrates using a continuous wave laser did lead to promising, but not to fully satisfactory, results [7]. Besides, in [11], a conductive paste based on carbon nanotube composites was successfully bonded to heat stabilized PET at 150 deg. C. Likewise, terminals of field effect transistors were effectively soldered to heat stabilized PET using a silver paste [14]. Furthermore, SnAgCu solder pixels were successfully applied by means of laser induced forward transfer approach, and reflowed onto PET substrates [15].

In order to cope with restricted thermal budgets for soldering purposes, a number of approaches exist. First, eutectic compounds, which conventionally melt at lower temperatures than the individual components that constitute the compound itself, are used as soldering mediums [17]. Further, localized soldering reduces thermal loading at the system level and focuses the application of heat exclusively to the region that is to be soldered [18]. In addition, since temperature sensitive materials exhibit an exponential increase in thermal expansion when thermally loaded, differential heating and cooling is proven to alleviate the effect of mismatches in thermal coefficients on the soldered product [19].

Based on the previously mentioned techniques, we propose a procedure for soldering 3D opto-electronics onto low T<sub>g</sub> polymers. In particular, we preserve available conventional processing tools inducing minimal modifications and special handling. Additionally, we enable a horizontally integrated supply chain that uses distinct suppliers and manufacturers for raw materials and components.

## Test Vehicle and Materials Characterization

We showcase our approach by manufacturing a test vehicle on a commercially acquired PET interposer. The interposer has the chemical composition  $[-C_{10}H_8O_4-]$ , a material density of 1,32 g/cm<sup>3</sup>, a VICAT softening point of 71 deg. C., and a melting temperature T<sub>m</sub> of 255 deg. C. Moreover, the interposer has a thickness of 200 μm. Furthermore, the ultimate tensile strength of the interposer is 45 N/mm<sup>2</sup>, and the tensile impact strength is 250 kJ/m<sup>2</sup>.

Copper (Cu) electronic interconnects of a thickness of 200 nm are sputter deposited on the PET interposer. Furthermore, 2 μm of Tin (Sn) are applied onto the region of the copper interconnects to-be-soldered through evaporation. Specifically, structuring of interconnects and soldering pads is achieved using a shadow mask. Particularly, the shadow mask is made of steel, structured means laser and 100μm thick.

In order to improve the adhesion of the electronic interconnects to the PET interposer by increasing the surface roughness and enhancing the purity of the surface, the interposer surface is subject to oxygen plasma treatment. Consequently, the roughness of the interposer is characterized by the arithmetic mean  $R_a=24.64$  nm, the quadratic mean  $R_q=34.81$  nm and the maximum roughness  $R_{a,max} = 36.03$  nm. However, no significant change in thickness is recorded. It is to be noted that the plasma treatment intentionally does not induce a lasting chemical activation of the surface.

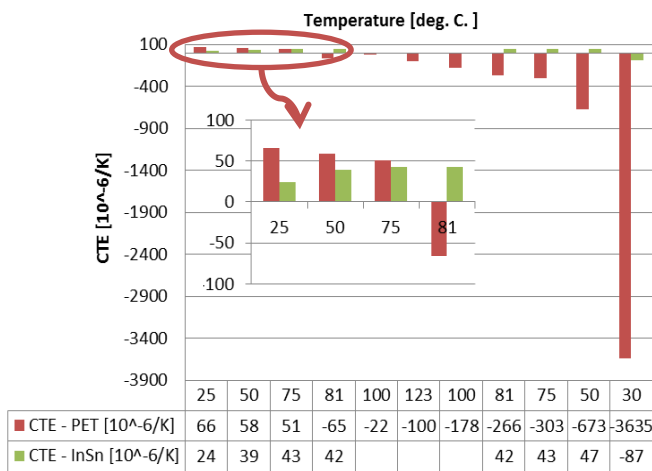


**Figure 1:** Coefficients of thermal expansions of PET and InSn measured during a heating and cooling cycle.

Empirically obtained, the chains of the PET film are observed to reversibly decay back to equilibrium once thermally loaded under 130 deg. C. for not more than a couple of seconds, which we refer to later as relaxation time.

A commercial top light emitting diode (LED) is soldered to the electronic interconnects. Notably, the LED is based on InGaN and packaged as a surface mount device in a plastic housing of the size 5.0x5.0x1.6 mm<sup>3</sup>. Pre-tinned copper legs connect the LED to the outside of the package. Besides, the LED can sustain up to 260 deg. C. in reflow soldering temperature for a duration of 4 seconds, and up to 80 deg. C. during ongoing operation. A maximum of 30 mA forward direct current operates the LED. Markedly, the test vehicle does not comprise a current-limiting serial resistor connected to the LED. Therefore, forward direct currents of the order of 0.5 mA are not to be surpassed.

A eutectic compound of 48 w. % Sn and 52 w. % Indium (In), later referred to as InSn, which is commercially available as a 50 μm thick ribbon, is employed for soldering the legs of the LED to the interconnects. In particular, the liquidus temperature of the solder lies at around 118 deg. C. Moreover,

the eutectic solder is characterized by a tensile strength of 11 N/mm<sup>2</sup> and shear strength of 11.2 MPa. Since soldering is conducted under ambient conditions, the use of soldering grease (DIN EN 23451-1 F-SW21 according to German Institute for Standardization) becomes necessary in order to break the oxide layers at interconnects and solder.

So far, the mentioned characteristic figures are obtained from the manufacturer or the distributor except the surface roughness data, which was obtained in house. Moreover, using an optical dilatometer, coefficients of thermal expansions of the PET film and the InSn ribbon were measured (Figure 1). As a matter of fact, the glass transition temperature of the PET film was verified to be less than 80 deg. C. In addition, the InSn material maintains a fairly constant coefficient of thermal expansion during the heating and cooling cycle. Furthermore, the mismatch of coefficients of thermal expansions between InSn and PET is alleviated when heated above 50 deg. C. and under the T<sub>g</sub> of PET.

Additionally, the PET film deforms exceedingly, and irreversibly, once completely subject to temperatures above 80 deg. C. Further, it is to be noted that large negative coefficients of thermal expansion are an indication for a curling of the free extremities of the sample, which is detected to be a shrinking of the material by the optical dilatometer.

### Setup of Eutectic Soldering

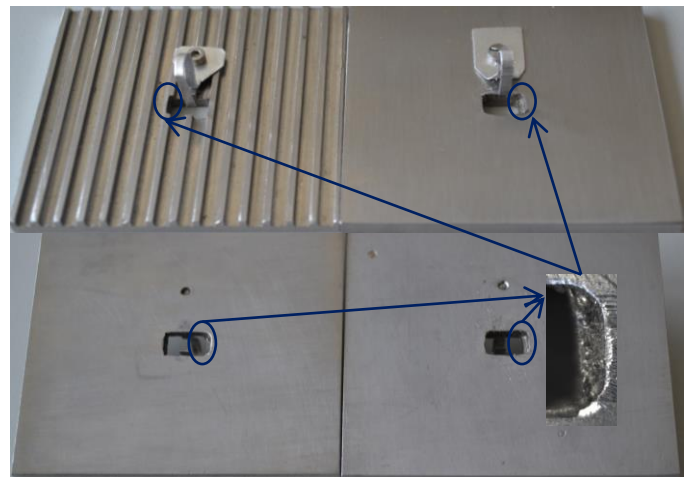


**Figure 2:** Metal jigs with and without grooves, hook/contact spring, and detail of flow chamber

Typically used for rework purposes, a focused hot air gun with a cylindrical vent with a diameter of 0.6 mm is used as a localized heat source for soldering purposes. The temperature of the hot air arriving at the region to-be-soldered depends on the distance of the opening of the hot air gun to the solder; and the angle with which the hot air collides. For instance, hot air emanating from the gun at a temperature of 250 deg. C. arrives at a temperature of 140 deg. C. after traveling a vertical distance of 1.5 centimeters. During soldering, the amount of hot air is measured and adjusted by means of a precision flow meter.

Next, a metal jig made of stainless steel with an aperture for the LED is used. In particular, the jig serves as a shield to protect the interposer surface outside the soldering zone from

thermal loading. In addition, the jig functions like an iron load to maintain planarity of the polymeric interposer. As importantly, the jig acts as a passive heat sink for accelerating heat dissipation by the polymer film. In this regard, two variants of the metal jig are investigated: (a) a homogeneous board with an aperture for LED, and (b) a homogeneous board with an aperture and pin fin enlarging the surface area of the jig (Figure 2). Moreover, both jigs dispose of a small flow chamber located at the corner of the LED aperture. Hence, hot air emanating from the air gun is trapped into the flow chamber and localized. In order to maintain contact between interconnects and LED during soldering, and in addition to avoiding chuck vacuum, a slender plate in the shape of a hook serves as a contact spring. Specifically, a light spring load becomes active once the hook is pushed down to touch the center of the upper surface of the LED. Consequently, contact between the LED and the polymer film is ensured during solder drop formation, solder wetting and thermal shrinkage. Last but not least, geometrical dimensions of jigs (60 mm x 35 mm x 4 mm), pins (1.25 mm x 2.5 mm), distance between pins (3.3 mm), and aperture (5.5 mm x 5.5 mm) were adopted.

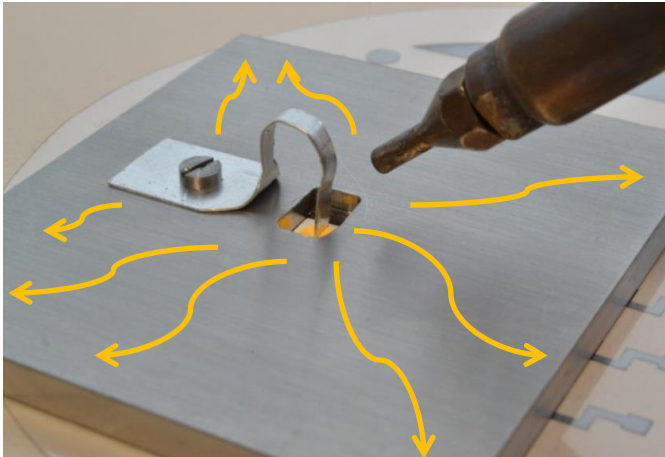


**Figure 4:** Soldering setup (Note: metallic platform is not depicted) and example of heat flow pattern

Differential heating and cooling are enabled through the use of a metallic platform, which is made of stainless steel and 7 mm thick, under the polymeric film. According to the coefficients of thermal expansion discussed in the previous section, and while the hot air is required to meet the melting temperature of the InSn eutectic compound, 118 (+20) deg. C., the configuration of the soldering setup is designed to facilitate the polymeric substrate to maintain low thermal expansion. During soldering, the temperature of the polymeric film around the soldering zone is verified using a digital quick-response thermocouple.

The soldering setup (Figure 4) is mounted under ambient conditions. The surrounding temperature is maintained at constant 21 deg. C. Relative humidity is kept within the range of 40-70%.

### Process of Eutectic Soldering

Using the setup described above, the LED is eutectically soldered according to the following procedure (Figure 3):

1. InSn ribbon is folded multiple times in order to attain the required amount of solder.
2. InSn is immersed in soldering grease.
3. InSn is positioned onto the Sn pads. Soldering grease works as a temporary mechanical fixation of InSn to the Sn pads.
4. LED is positioned on the polymer film and fixed prior to soldering by instant bonding of the bottom face of the LED to the polymer film. Conventional cyanoacrylate adhesive is used.
5. Soldering jig is applied on the test vehicle with LED located in the aperture of the jig.
6. Contact spring/hook is applied on the LED.
7. Hot air vent is focused at soldering region at an angle of 45 degrees.
8. Hot air flow is set to required level.
9. Hot air is released in 2 second pulses, which is less than the relaxation time of the PET.
10. Hot air is released again once temperature of polymer is reset to 21 deg. C, i.e. heat is dissipated from soldering zone through jig and metallic platform. Temperature is verified using the thermocouple.
11. Repeat steps 9 and 10 until solder drop formation is complete.

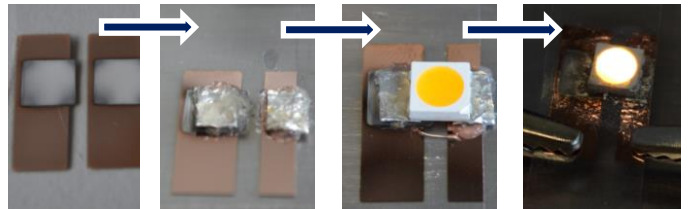


**Figure 3:** Process order (from left to right: (1) Cu interconnects and Sn pads, (2) deposition of folded InSn ribbon immersed in soldering grease, (3) instant bonding of LED, (4) LED in operation after soldering)

### Results and Discussion

Besides from successful operation of the LED under direct current, optical inspection of the soldering zone discloses successful wetting and formation of intermetallic

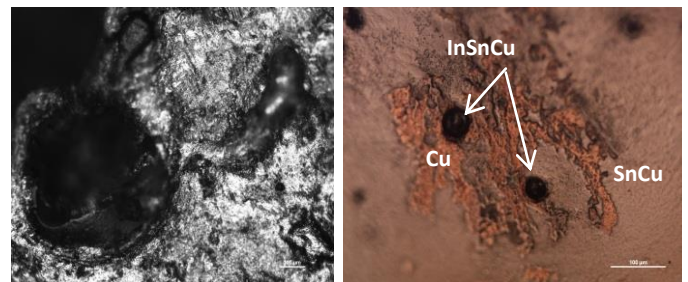


**Figure 5:** Top view of solder wetting on Sn pads (left), Bottom view through transparent polymer of formation of inter-metallic phases between Sn, Cu and InSn (right)

phases between interconnects, solder and pads (Figure 5).

Soldered regions remain connected after thermal shrinkage, which is an indication for acceptable stresses within the assembly.

Due to low thickness (200 nm) of Cu, microscopic inspection of interconnects before and after soldering enable the investigation of material deformation inside and outside of soldering zone. Apart from handling aftereffects, e.g. scratches through tweezers, the Cu layer remains intact after soldering (Figure 7). In particular, formation of micro-cracks does not occur.

Measurements of temperature during soldering reveal that the temperature gradient decays rapidly over the soldering region constraining the soldering zone to minimal CTE mismatches. Therefore, the soldered product exhibits minimal warpages. Moreover, the use of soldering jig is proven to be beneficial by shrinking the heat affected zone. Average diameters of heat affected zones for variations of usage of soldering jig are listed in Table 1.

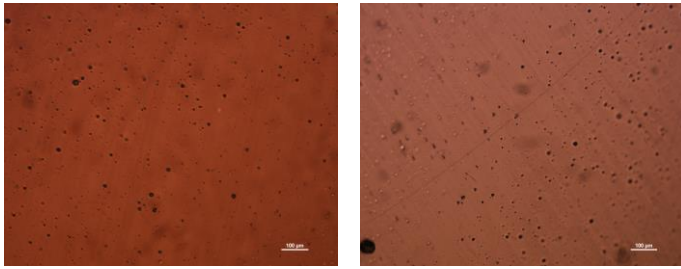


**Figure 7:** Cu interconnects before (left) and after (right) soldering (Note: different regions are depicted)

The chemical reaction between soldering grease and PET is investigated by subjecting the PET-soldering grease assembly to thermal testing at 60 deg. C., in particular below glass transition of PET, for about 2 hours. Despite ultrasonic cleaning in an ethanol bath, residues of the soldering grease remain on the surface of the PET film (Figure 6), which is a clear indication for a thermo-chemical reaction between soldering grease and PET. In this regard, either compatible soldering grease should be determined or soldering grease should be completely eliminated from the assembly. In the latter case, special care needs to be taken in order to avoid oxidation of interconnects and solder.

	Without jig	Jig	Jig with fin
Diameter	8 mm	5 mm	2 mm

**Table 1:** Diameter of heat affected zone for various usage of jig at 118 (+20) deg. C. and after 10 seconds

Even though cyanoacrylate adhesive is used for temporary mechanical fixation and is not needed any longer after soldering is complete, it is significant to consider the chemical degradation of the adhesive due to thermal loading during soldering. Here, deterioration of the instant adhesive is not observed due to low soldering temperature and short thermal loading. In terms of mechanical bendability, the flexibility of the system is prohibited at the contact region between LED and interposer.

The amount of hot air required for soldering depends on the soldering setup and product, in particular materials and geometry. For the test vehicle presented in this work, a hot air flow of 1792 sccm is determined to be optimal. On one hand, smaller amounts of hot air are observed to be dissipated quickly, and so solder drop formation does not occur. On the other hand, larger amounts of hot air take longer to be

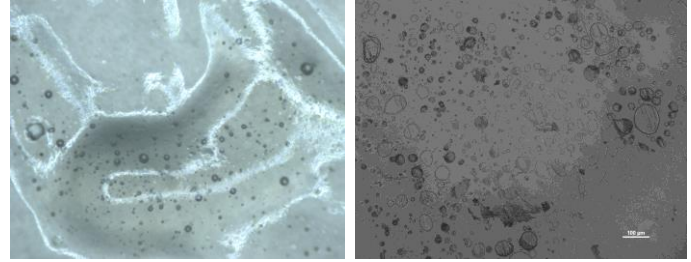


**Figure 6:** Grease drop on PET before thermal testing (left), Residues of soldering grease on bare PET after thermal testing and cleaning (right)

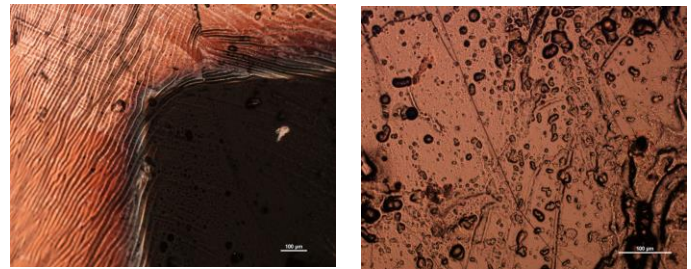


**Figure 8:** Sand dune effect (left), Blown solder and grease particles (right)

dissipated, and the polymer relaxation time is consequently exceeded.

The use of hot air induces side effects. First, hot air can arrive at regions outside of soldering zone, and cause the formation of sand dunes of material (Figure 8). Second, particles of solder and soldering grease can be blown outside of soldering region by hot air, which may cause short circuits. By maintaining perfect contact between the soldering jig and the polymer film, these artifacts can be easily avoided.

In terms of manufacturing costs, while InSn is more expensive than classical solders such as SnCu, the solder cost is substantially compensated by the inexpensive interposer. Moreover, the investment of soldering setup, i.e. the soldering jig and metallic plate, can be counterbalanced by roll-to-roll mass production. It is to be noted that the size of the aperture is dependent on the component and combination of components on the board as well.

## Conclusion

We developed an inexpensive and reproducible assembly approach for 3D components onto low Tg polymers based on four principles:

- (1) Localized application of heat,
- (2) Low temperature eutectic soldering,

- (3) Differential heating and cooling,
- (4) Ironing during heating and thermal shrinkage.

We successfully demonstrated a test vehicle based on PET, which has a T<sub>g</sub> of 71 deg. C. Notably, solder wetting and formation of inter-metallic phases prevailed. Moreover, the heat affected zone was minimized, such that interposer warpage was limited.

### Acknowledgments

The authors gratefully acknowledge the financial support by Deutsche Forschungsgesellschaft (DFG) within the Collaborative Research Center "Transregio 123-Planar Optronic Systems."

Moreover, the authors would like to acknowledge Prof. Schade and Elke Pichler from the Institute of Energy Research and Physical Technologies at the Technical University of Clausthal for coordinating the measurements of the coefficients of thermal expansion.

### References

1. Jeong In Han, 2003, "Flexible Display; Low Temperature Processes for Plastic LCDs", Transactions on Electrical and Electronic Materials, vol. 4, pp. 10-14.
2. S. Cichos, J. Haberland, H. Reichl, "Performance Analysis of Polymer based Antenna-Coils for RFID", Proc. IEEE Polytronic, 2002, pp. 120-124.
3. K. Koski, J. Hölsä, P. Juliet, Z.H. Wang, R. Aimo, K. Pischow, 1999, "Characterization of aluminum oxide thin films deposited on polycarbonate substrates by reactive magnetron sputtering", Materials Science and Engineering: B, vol. 65, issue 2, pp. 94-105.
4. F. Bodino, G. Baud, M. Benmalek, J.P. Besse, H.M. Dunlop, M. Jacquet, 1993, "Alumina Coating on polyethylene terephthalate", 1994, Thin Solid Films, vol. 241, pp. 21-24.
5. Manal M. Shalabi, Johannes G.C. Wolke, Vincnet M. J.I. Cuijers, John A. Jansen, 2007, "Evaluation of bone reponse to titanium-coated polymethyl methacrylate resin (PMMA) implants by X-ray tomography", Journal of Materials Science: Materials in Medicine, vol. 18, pp. 2033-2039.
6. Ana Maria Oliveira Brett, Frank Michael Matysik, M. Teresa Vieira, 1997, "Thin-film gold electrodes produced by magnetron sputtering. Voltammetric characteristics and application in batch injection analysis with amperometric detection", Electroanalysis, Vol. 9, pp. 209-212.
7. Jussi Putaala, Maciej Sobocinski, Saara Ruotsalainen, Jari Juuti, Petri Laakso, Heli Jantunen, 2014, "Characterization of laser-sintered thick film paste on polycarbonate substrates", Optics and Lasers in Engineering, vol. 56, pp. 19-27.
8. W. A. MacDonald, M. K. Looney, D. MacKerron, E. Eveson, R. Adam, K. Hashimoto, K. Rakos, 2012, "Latest advances in substrates for flexible electronics", Journal of the Society for Information Display, vol. 15, pp. 1075-1083.
9. Frederik C. Krebs, Mikkel Jorgensen, Kion Norrman, Ole Hagemann, Jan Alstrup, Torben D. Nielsen, Jan Fyenbo, Kaj Larsen, Jette Kristensen, 2009, "A complete process for production of flexible large area polymer solar cells entriely using screen printing – First public demonstration", Solar Energy Materials and Solar Cells, vol. 93, pp. 422-441.
10. Seung-Ho Kim, Kiwon Lee, Kyung-Wook Paik, 2010, "High speed touch screen panels (TSPs) assembly using anisotropic conductive adhesives (ACAs) vertical ultrasonic bonding", 60<sup>th</sup> proceedings of IEEE Electronic Components and Technology Conference (ECTC), pp. 1964-1967
11. J.H. Choi, J.H. Park, J.S. Moon, J.W. Nam, J.B. Yoo, C.Y. Park, J.H. Park, C.G. Lee, D.H. Choe, 2006, "Fabrication of carbon nanotube emitter on the flexible substrate", Diamond and Related Materials, vol. 15, pp. 44-48
12. G. Connell, R. L. D. Zenner, J. A. Gerber, 1997, "Conductive adhesive flip-chip bonding for bumped and unbumped die", Proceedings of 47th IEEE Electronic components and Technology Conference, pp. 274-278.
13. Lin Hui, Yu Junsheng, Wang Nana, Huang Chunhua, 2008, "Flexible organic light-emitting diodes with improved performance by insertion of an UV-sensitive layer", Journal of Vacuum Science and Technology B: Microelectronics and Nanometer Structures, vol. 26, pp. 1379-1381.
14. B. Nalini, D. Nirmal, J. Cyril Robinson Azriah, 2013, "Fabrication and characteristics of flexible thin film depletion mode field effec transistor (FET) using high k dielectric nano zirconia", International Journal of Emerging Trends in Engineering and Development, vol. 2, pp. 295-299.
15. K.S. Kaur, J. Missine, B. Vandecasteele, G. Van Steenberge, S.M. Perinchery, E.C.P. Smits, R. Mandamparabil, 2013, "Laser-induced forward transfer-assisted flip-chip bonding of optoelectronic components", IEEE Conference on Lasers and Elecro-Optics-International Quantum Electronics Conference, Abstracts.
16. Yinxiang Lu, Suhua Jiang, Yongming Huang, 2010, "Ultrasonic-assisted electroless deposition of Ag on PET fabric with low silver content for EMI shielding", Surface and Coatings Technology, vol. 204, pp. 2829-2833
17. J. Glazer, 1994, "Metallurgy of low temperature Pb-free solders for electronic assembly", International Materials Reviews, vol. 40, pp. 65-93
18. Y.T. Cheng, L. Lin, K. Najafi, 1999, "Localized bonding with PSG or indium solder as intermediate layer", 12<sup>th</sup> IEEE International Conference on Micro Electro Mechanical Systems, pp. 285-289.
19. K. Sakuma, E. Blackshear, K. Tunga, Lian Chenzhou, Li Shidong, M. Interrante, O. Mantilla, Jae-Woong Nah, 2013, "Flip chip assembly method employing differential heating/cooling for large dies with coreless substrates", IEEE 63<sup>rd</sup> Electronic Components and Technology Conference, pp. 667-673.

20. Jongman Kim, Harry Schoeller, Junghyun Cho, Seungbae Park, 2007, "Effect of oxidation on indium solderability", *Journal of Electronic Materials*, vol. 27, pp. 483-489.